Available online at www.sciencedirect.com
ScienceDirect
Journal of Molecular Catalysis A: Chemical 275 (2007) 200–205
JOURNAL OF MOLECULAR CATALYSIS A: CHEMICAL
www.elsevier.com/locate/molcata

# Effect of Pt/Pd-doped $TiO_2$ on the photocatalytic degradation of trichloroethylene

Hsin-Hung Ou, Shang-Lien Lo *

*Research Center for Environmental Pollution Prevention and Control Technology, Graduate Institute of Environmental Engineering, National Taiwan University, 71 Chou-Shan Rd., Taipei 106, Taiwan, ROC*

Received 5 March 2007; received in revised form 26 May 2007; accepted 29 May 2007
Available online 7 June 2007

**Abstract**

Photocatalytic degradation of trichloroethylene (TCE) over Pt/Pd-doped $TiO_2$ was conducted to investigate the effect of Pt and Pd on the TCE degradation and on the yields of dichloroacetyl chloride (DCAC) and phosgene. In the presence of Pt and Pd, the degradation of TCE was retarded; especially Pd had a significantly negative effect on TCE degradation, which was ascribed to the intercalation of Pd into the lattice of $TiO_2$. Moreover, Pt had no influence on the selectivity toward DCAC and phosgene while the selectivity toward phosgene in the presence of Pd was enhanced. As for the behavior of Pt and Pd in TCE degradation, Pt-doped $TiO_2$ exhibited the same photocatalytic behavior as P25 $TiO_2$ whereas Pd-doped $TiO_2$ led to a different photocatalytic mechanism.


*Keywords:* Metal-doped $TiO_2$; Trichloroethylene

## 1. Introduction

Photocatalysis has been a promising and significant prospect for environmental purifications where it is confirmed that the photocatalytic potential is subject to the recombination of generated photoelectrons and photoholes. To improve the photocatalytic efficiency in this regard, many studies have conducted a variety of modifications aimed at the crystal structure, specific surface area, doping species, surface hydroxyl group and so on. Among these modifications, metal doping has been found to enhance the photocatalytic performance efficiently and to change the photocatalytic mechanism. Such enhancement is ascribed to several origins. Firstly, the formation of Schottky barrier at the interface of metals and $TiO_2$ improves the separation of holes and electrons. Secondly, the holes act as a sink for electrons to prevent the accumulation of excess electrons on the surface of $TiO_2$. Thirdly, the defect sites ($Ti^{3+}$), which are responsible for the potential of photocatalysis, can be enhanced by some metal particles. However, the reported doped metals do not always have a positive effect on the improvement of photocatalytic efficiency and the role of doped species in reaction mechanism is far more complex than being a simple electron sink [1–4].

Trichloroethylene (TCE), a well-known volatile organic compound, has been applied to various industrial uses such as degreasing and dry cleaning. Such applications of TCE have become one of the major concerns in environmental pollution. Photocatalytic oxidation of TCE has been confirmed as an efficient treatment, and Dibble and Raupp [5] first reported the photocatalytic oxidation of TCE over $TiO_2$. Subsequent studies have revealed the degradation behavior of TCE in terms of reaction conditions and the degradation mechanism has also been well explained [6–17]. In general, photocatalytic degradation of TCE over $TiO_2$ produces two major by-products, dichloroacetyl chloride (DCAC) and phosgene, along with trace amounts of pentachloroethane ($C_2HCl_5$), oxalyl chloride (COClCOCl), and monochloroacetic acid ($CH_2ClCOOH$, MCAA). However, little attention has been paid to the effect of metal-doped $TiO_2$ on photocatalytic degradation of TCE. Driessen and Grassian [2] investigated the photocatalytic oxidation of TCE over Pt/$TiO_2$, and discovered that Pt species retards the degradation of TCE. Park et al. [3] have also tested several types of doped metal, and concluded that the high valence cations ($Mo^{5+}$, $Nb^{5+}$, and $W^{6+}$) improved TCE degradation owing to the relatively high amount

* Tel.: +886 2 23625373; fax: +886 2 23928830.
*E-mail address:* sllo@ntu.edu.tw (S.-L. Lo).

1381-1169/$ – see front matter © 2007 Elsevier B.V. All rights reserved.
doi:10.1016/j.molcata.2007.05.044

of adsorbed hydroxyl group. The effect of Cr, Fe, Ni, Cu, Pt and $Ca(OH)_2$ on the formation of DCAC, phosgene, and chloroform was also investigated by Tanimura et al. [4], showing that the by-products from photocatalytic degradation of TCE could be suppressed by the addition of Cu and $Ca(OH)_2$. Therefore, the present study attempted to examine TCE degradation over Pt/Pd-doped $TiO_2$. The yields of DCAC and phosgene were also measured to investigate the effect of Pd and Pt on the selectivity toward DCAC and phosgene. A plausible mechanism of TCE degradation in the presence of Pt/Pd species was also proposed.

## 2. Experiment

### 2.1. Preparation of Pt-doped $TiO_2$ and Pd-doped $TiO_2$

The modified $TiO_2$ were prepared by the impregnation method. 600 mg $TiO_2$ (Degussa P25) were stirred in a series of concentrations of $H_2PtCl_6$ and $PdCl_2$ solutions at 373 K for 60 min. Afterward, the resulting $Pt^{4+}/TiO_2$ and $Pd^{2+}/TiO_2$ slurries were dried in a vacuum freeze-dryer for 20 h (100–200 mTorr at −57.5 °C). Pt-doped $TiO_2$ and Pd-doped $TiO_2$ samples were obtained in the tubular oven under the atmosphere of 20% $H_2$/80% $N_2$ at progressively elevated temperatures for 3 h (30, 120, and 400 °C). The as-prepared Pt-doped $TiO_2$ and Pd-doped $TiO_2$ were exposed to the air for 3 hr before further characterizations, an exposure period similar to that during the kinetic experiments. In the following passages, Pt-doped $TiO_2$ and Pd-doped $TiO_2$ reduced at 400 °C is abbreviated as $Pt/TiO_2$ and $Pd/TiO_2$, respectively.

### 2.2. Characterization of Pt-doped $TiO_2$ and Pd-doped $TiO_2$

BET specific surface areas ($S_{BET}$) of the samples were measured by an automated gas adsorption analyzer (Micromeritics ASAP 2010). X-ray diffraction (XRD) with the scan range of 20–80° was employed to determine the crystalline phase of the modified $TiO_2$ powders. X-ray photoelectron spectroscopic (XPS) analysis was carried out on a spectrometer equipped with a Mg (Kα) X-ray source. All binding energies were referenced to the C 1s peak at 284.6 eV, which is invariably present on the film surface. The spectra were fitted by XPSPEAK with a linear background and to 80% Gausssian/20% Lorentzian peak shape. The standard procedure of temperature programmable reduction (TPR) measurements involved purging the reactor with He gas for 30 min, and heating the powders at 150 °C for 60 min to remove the impurities and water adsorbed on the surface of modified $TiO_2$. The resulting powders were subsequently reduced by a mixing gas of 90% Ar/10% $H_2$ at 40 ml $min^{-1}$ and a temperature ramping rate of 10 °C $min^{-1}$ from 25 to 600 °C. The structure of anatase $TiO_2$ demonstrated in the manuscript was constructed by the Ca.R.Ine version 3.1 crystallography program package.

### 2.3. Photocatalytic tests

Batch experiments of photocatalytic degradation of TCE were conducted in a flat-plate photoreactor (FPPR). This reactor was made of stainless steel with a volume of 2 L ($L$ = 20 cm, $W$ = 10 cm, and $H$ = 10 cm), both ends to which silica wafer was adhered to avoid emission. The detail was described in our previous publication [17]. $TiO_2$, Pt-doped $TiO_2$, and Pd-doped $TiO_2$ samples supported on silica board of 120 $cm^2$ were prepared by the dip-coating method with a normalized concentration of 0.83 mg $cm^{-2}$. For a typical run, the initial concentration of TCE was 67.7 ± 5 μM, and the relative humidity and oxygen concentration were kept at 25 ± 2.5% and 3.53 mM, respectively. The reactor was wrapped with a heating tape to maintain a temperature of 308 K. Illumination was provided by three 8 W black-light fluorescent lamps, principally emitting a light 365 nm in wavelength with an intensity of 2.34 ± 0.23 mW $cm^{-2}$. TCE, DCAC, and phosgene were quantified under a series of time sequence via manual injection into a gas chromatograph (5890II) equipped with a flame ionization detector. The photocatalytic ability of doped $TiO_2$ was surveyed by the observed rate constant ($k_{obs}$) of TCE degradation based on the pseudo-first-order reaction.

## 3. Results and discussion

### 3.1. Specific surface area and XRD analysis

No significant change in $S_{BET}$ was observed among the modified $TiO_2$ samples and the values fell into the range of 47–52 $m^2$ $g^{-1}$. Compared to the $S_{BET}$ of P25 $TiO_2$ (52.5 $m^2$ $g^{-1}$), a slight decrease with increasing loading amounts of Pt and Pd was found. The phenomenon can be attributed to the aggregation of $TiO_2$ after thermal treatment and the blocking of fine capillaries of the parent $TiO_2$ surface by metal islands. Moreover, neither $Pt/TiO_2$ nor $Pd/TiO_2$ presented obvious change in XRD spectra (Fig. 1). This result can presumably be ascribed to the combinations of low contents of doping Pt or Pd, small particle size, and homogeneous distribution.

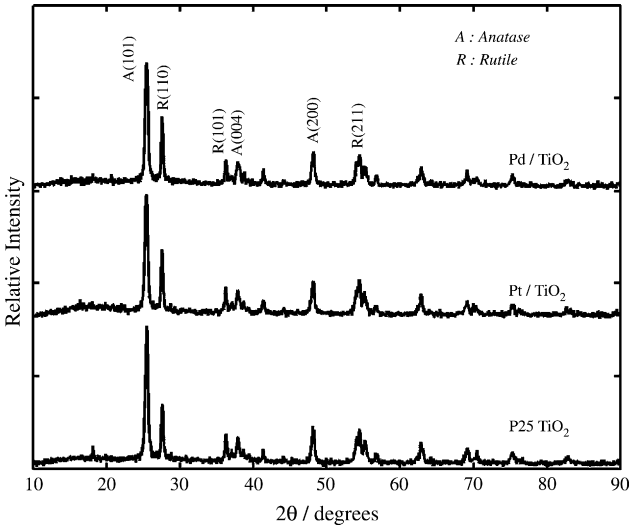


Fig. 1. The XRD patterns of P25 $TiO_2$, 0.1 wt.% $Pt/TiO_2$ and 0.04 wt.% $Pd/TiO_2$.

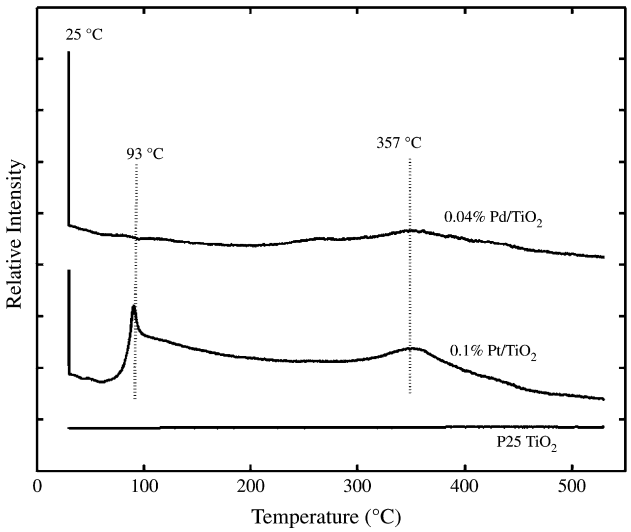


Fig. 2. The TPR spectra of P25 $TiO_2$, 0.1 wt.% Pt $TiO_2$ and 0.04 wt.% Pd $TiO_2$.

### 3.2. TPR

Fig. 2 demonstrates TPR spectra concerning the reduction scenario of $K_2PtCl_4$ and $PdCl_2$. No significant peak for pure $TiO_2$ was observed in the temperature of interest ranging from 25 to 600 °C. In the case of the representative Pt-doped $TiO_2$, the TPR profile exhibited an obvious peak at room temperature along with two other peaks at 93 and 357 °C. The phenomenon suggests the presence of three stages during the reduction process. The first peak exhibits the highest intensity, whereas the second peak amounts to one-third of the hydrogen consumption. This indicates the majority of Pt species is reduced to $Pt^0$ at room temperature. The TPR spectrum of Pd-doped $TiO_2$ presented a significant peak at 25 °C, with a vague peak at approximately 355 °C, also indicating that the Pd species can be reduced to $Pd^0$ at room temperature in the presence of $H_2$. Besides, the color of the Pt-doped $TiO_2$ and Pd-doped $TiO_2$ samples changed from bright yellow and reddish to gray, respectively, suggesting that the surface species on $TiO_2$ have been changed.

### 3.3. XPS

XPS analysis was conducted to determine the chemical and electronic structure of the as-prepared samples. The XPS spectra of O 1s within $TiO_2$ can be principally assigned to the crystal lattice oxygen ($Ti^{4+}$–O) and surface adsorbed OH (Ti–OH) with the binding energies of 529.8 and 531.3 eV, respectively [18]. Fig. 3(a and b) show the deconvoluted O 1s bands of Pt/$TiO_2$ and Pd/$TiO_2$, respectively, which indicate the presence of $Ti^{4+}$–O and Ti–OH. As seen in Table 1, the concentration of Ti–OH increases after the modification by Pt and Pd doping, suggesting the doped $TiO_2$ enhance the formation of $OH^{\bullet}$. Regarding the Ti species for Pt/$TiO_2$ and Pd/$TiO_2$, curve fitting indicated the presence of $Ti^{3+}$ in addition to the dominant $Ti^{4+}$ peak (Fig. 3(c)). This evidenced the existence of reduced states ($Ti^{3+}$) with the line position at 457.5 eV, while the bonding energy of $Ti^{4+}$ is located at 459 eV. The formation of $Ti^{3+}$ implies that the interaction between Pt/Pd species and $TiO_2$ matrix occurred during the reduction reaction [19]. $Pt^{II}$ was the major species after reduction at 25 and 120 °C, while $Pt^0$ was dominant in the case of samples reduced at 400 °C (Fig. 4(a)). This indicates that the successive reduction from $Pt^{IV}$ to $Pt^0$ needs to be driven at 400 °C. As seen in Fig. 4(b), oxidation species of Pd was also observed at 25 and 120 °C, even though the TPR result demonstrated that the majority of Pd species can be reduced to $Pd^0$ at 25 °C. In fact, there is a discrepancy in the Pt/Pd amount between the XPS results and theoretical introduction in fabrication. This indicates that part of the introduced Pt/Pd is not on the surface of $TiO_2$, and suggests the intercalation of Pt and Pd into the lattice of $TiO_2$. In addition, the peak shift was observed in the cases of Pt/$TiO_2$ and Pd/$TiO_2$, which can be ascribed to either diameter change of Pt/Pd particles or the charge transfer from the partially reduced $TiO_x$ to Pt/Pd particles [20–22].

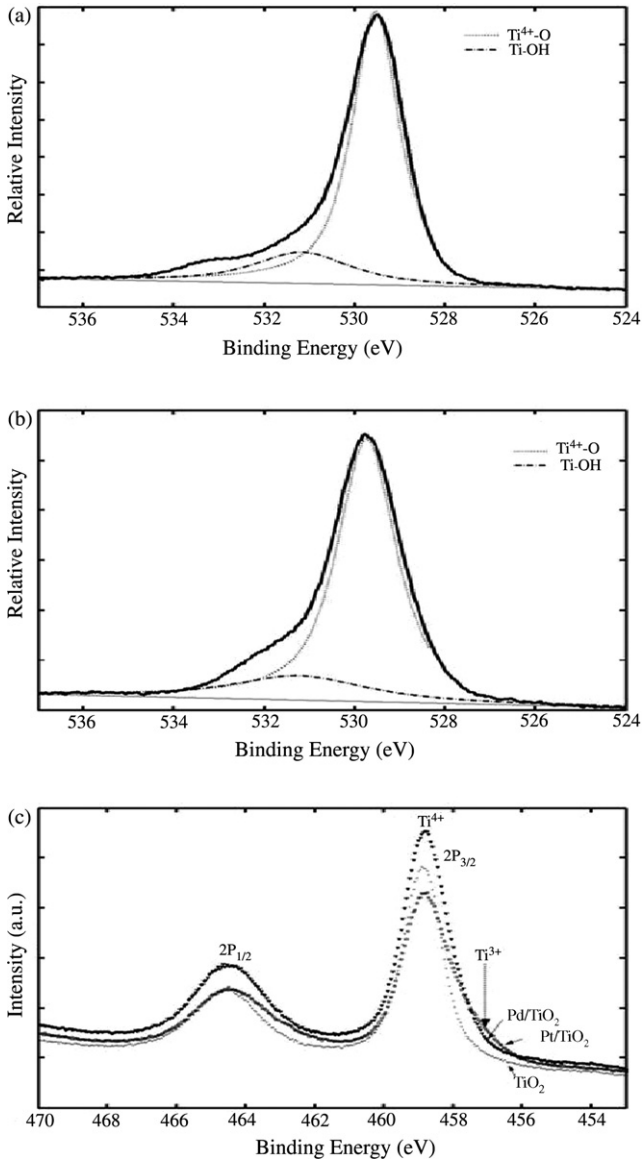


Fig. 3. The XPS spectra of (a) 0.1 wt.% Pt/$TiO_2$ for O 1s region, (b) 0.04 wt.% Pd/$TiO_2$ for O 1s region and (c) P25 $TiO_2$, 0.1 wt.% Pt/$TiO_2$ and 0.0 wt.% Pd/$TiO_2$ for Ti 2P region.

Table 1
Results of curve-fitting of high resolution XPS spectra for the O1s region in Pt-doped $TiO_2$ and Pd-doped $TiO_2$

| Catalysts | Crystal lattice oxygen ($Ti^{4+}$—O) | | Surface adsorbed OH (Ti—OH) | |
|---|---|---|---|---|
| | Peak area (%) | Binding energy (eV) | Peak area (%) | Binding energy (eV) |
| Pure $TiO_2$ | 91.75 | 529.81 | 8.25 | 531.64 |
| 0.03 wt.% Pt/$TiO_2$ | 90.18 | 529.76 | 9.82 | 531.60 |
| 0.1 wt.% Pt/$TiO_2$ | 86.90 | 529.43 | 13.10 | 531.25 |
| 0.15 wt.% Pt/$TiO_2$ | 84.87 | 529.80 | 15.13 | 531.99 |
| 0.02 wt. Pd/$iO_2$ | 92.95 | 529.91 | 7.05 | 531.59 |
| 0.04 wt.% Pd/$TiO_2$ | 90.47 | 529.68 | 9.53 | 531.68 |
| 0.06 wt.% Pd/$TiO_2$ | 88.81 | 529.77 | 11.19 | 532.15 |

### 3.4. Catalytic tests

#### 3.4.1. The effect of Pt and Pd on TCE degradation

Compared with P25 $TiO_2$, Pt/$TiO_2$ and Pd/$TiO_2$ show poor performance in TCE degradation, as demonstrated in Fig. 5. In the case of Pt/$TiO_2$, the values of $k_{obs}$ fell into the range of $(1.02–1.62) \times 10^{-2}\,min^{-1}$ while that of P25 $TiO_2$ was $(1.70 \pm 0.08) \times 10^{-2}\,min^{-1}$. Concerning the performance of Pd/$TiO_2$, the corresponding $k_{obs}$ values fell into the range of $(0.40–0.79) \times 10^{-2}\,min^{-1}$, which were remarkably inferior to that of P25 $TiO_2$. The diminished activity can be attributed to many potential origins. The deposited Pt or Pd clusters would reduce the opportunities for TCE to adsorb on $TiO_2$ and would scatter the UV light to decrease the irradiation efficiency of $TiO_2$. Another reasonable inference is that the deposited metal particles may act as the recombination center for photoinduced holes

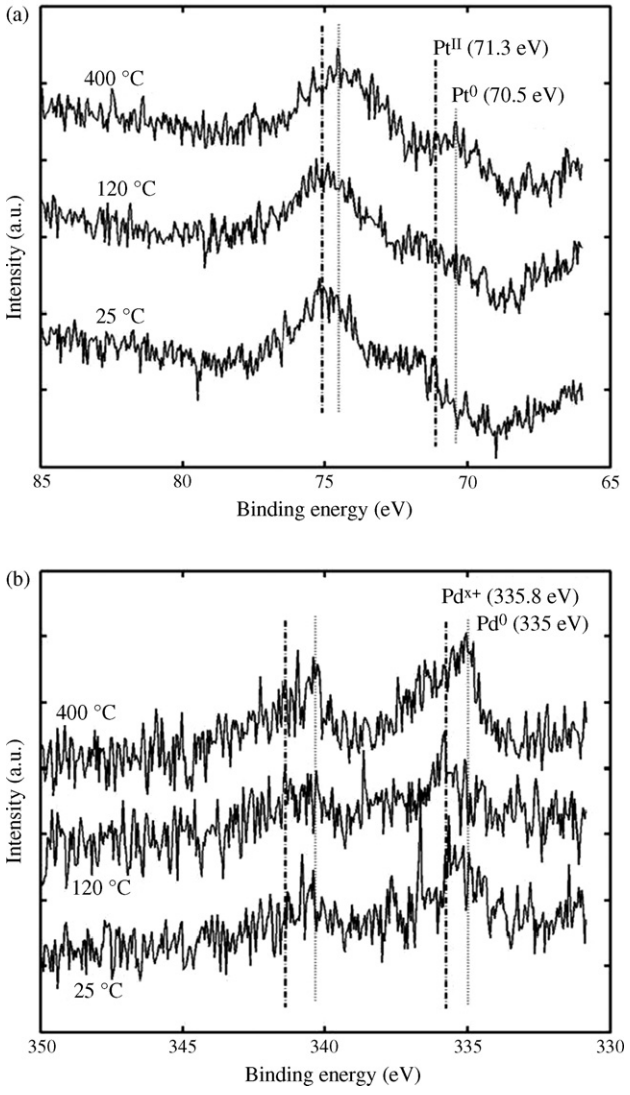


Fig. 4. The XPS spectra of (a) 0.1 wt.% Pt $TiO_2$ for Pt 4f region and (b) 0.04 wt.% Pd $TiO_2$ for Pd 3d region at reducing temperatures of 25, 120, and 400 °C.

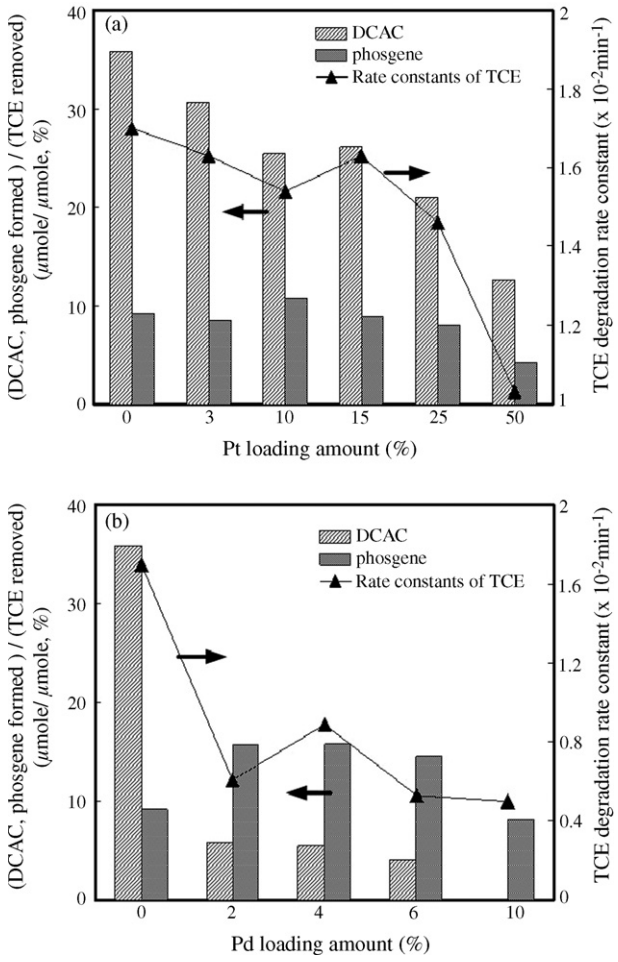


Fig. 5. The dependence of degradation rate constants of TCE, the yields of DCAC and phosgene on the loading amount of Pt/Pd species (a) Pt/$TiO_2$ and (b) Pd/$TiO_2$.

and electrons. The defect sites ($Ti^{3+}$) within catalysts were found to arise from the modification of Pt and Pd doping (Fig. 3(c)). However, the existence of $Ti^{3+}$ does not seem beneficial to TCE degradation even though it is possible for the adsorption and photoactivation of oxygen to produce $O_2^{\bullet -}$. Driessen and Grassian [2] reported that the presence of Pt particles was detrimental to the photocatalysis of TCE owing to the blocking of $Ti^{3+}$ active sites by Pt particles.

Regarding the major oxidant species in TCE degradation, some reports claimed that $OH^{\bullet}$ [3,14] were responsible for TCE degradation while others preferred $Cl^{\bullet}$ [4,6,7]. Table 1 demonstrates that the concentration of surface adsorbed OH increases with increasing loading amounts of Pt and Pd. However, the degradation rate of TCE was irrelevant to the concentration of OH, indicating that the $OH^{\bullet}$ may not account for the TCE degradation. Based on O-atom isotope-label studies, Fan and Yates [23] have also suggested that the surface adsorbed water was not involved in the TCE degradation. Therefore, it is confirmed that $Cl^{\bullet}$ instead of $OH^{\bullet}$ are responsible for TCE degradation.

In addition, the $k_{obs}$ values of $Pt/TiO_2$ samples were higher than that of $Pd/TiO_2$ by a factor of 1.5–4. The drastic decrease in the presence of Pd can be attributed to the intercalation of Pd into $TiO_2$ lattice. As shown in the XRD results (Fig. 1) no separate dopant-related phase is present. This indicates the dopant (Pt and Pd) is either dissolved within the substitution sites within the $TiO_2$ lattice or intercalated into the octahedral sites [19]. Meanwhile, the effective ion sizes of $Ti^{4+}$, $Pt^{4+}$, and $Pd^{2+}$ are 0.605, 0.625, and 0.86 Å, respectively. This suggests that $Pd^{2+}$ ion is energetically favorable to going into the larger octahedral interstitial sites in the $TiO_2$ lattice [24], as illustrated in Scheme 1. When $Pd^{2+}$ ion is doped into the $TiO_2$ lattice, the empty space within the lattice is reduced. The mobility of oxygen vacancies is then retarded and cannot reach the interior region of the $Pd/TiO_2$. Therefore, a far lower efficiency of electrons trapping for the $Pd/TiO_2$ significantly inhibits the formation of $Cl^{\bullet}$ (Eq. (2)), a principal oxidation species in TCE degradation.

### 3.4.2. The effect of reduction temperature of Pt/Pd species on TCE degradation

The effect of reduction temperature of Pt/Pd species on TCE degradation was also investigated with samples of

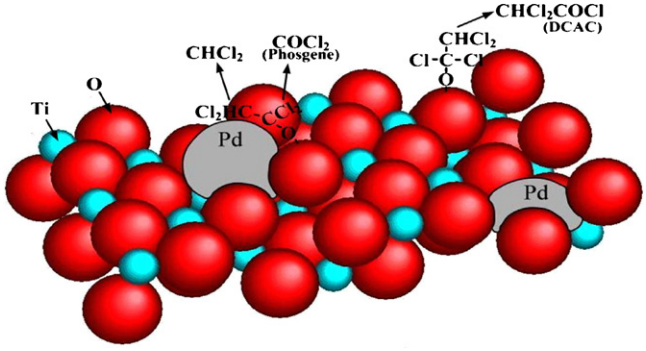


Scheme 1. $Pd/TiO_2$ surface. Pd species were intercalated into the lattice of $TiO_2$ and aided the cleavage of C—C bond within $CHCl_2COCl_2^{\bullet}$.

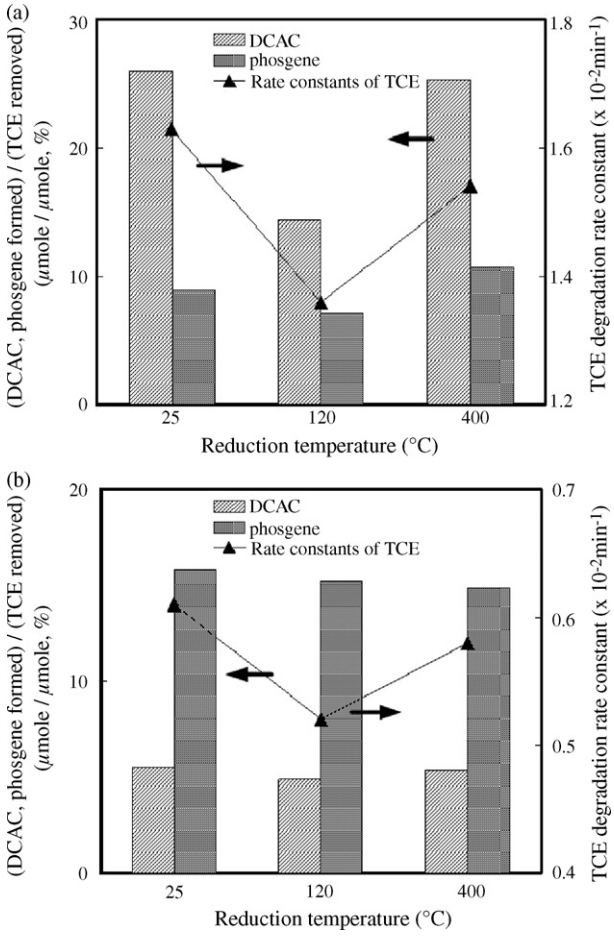


Fig. 6. The dependence of degradation rate constants of TCE, the yields of DCAC and phosgene on the reduction temperature of Pt/Pd species (a) 0.1 wt.% $Pt/TiO_2$ and (b) 0.04 wt.% $Pd/TiO_2$.

0.1 wt.% Pt-doped $TiO_2$ and 0.04 wt.% Pd-doped $TiO_2$ chosen for this measurement. Both Pt/Pd-doped $TiO_2$ samples revealed the photocatalytic ability following the order of 25 °C ≒ 400 °C > 120 °C (Fig. 6). Pt/Pd-doped $TiO_2$ reduced at 120 °C presented the minimum $k_{obs}$, which can be attributed to the existence of oxidation state of Pt/Pd (Fig. 4) because they provide an additional recombination center of irradiated electrons and holes [25]. Moreover, Pt/Pd-doped $TiO_2$ reduced at 120 and 400 °C were expected to possess lower $S_{BET}$ than that of samples reduced at 25 °C. That explains why samples reduced at 25 °C demonstrated the best performance on TCE degradation even though the oxidation state of Pt/Pd was predominant in Pt/Pd-doped $TiO_2$. Regarding the effect of oxidation state of Pt/Pd on byproducts, the yields of DCAC and phosgene in the presence of Pt correspond to the degradation rate of TCE (Fig. 6(a)) while Pd had no influence on it (Fig. 6(b)). The related mechanism is discussed in the following section.

### 3.4.3. The effects of Pt and Pd on the formation of DCAC and phosgene

The effects of Pt and Pd on the yields of DCAC and phosgene are demonstrated in Fig. 5(a and b), respectively, where the yield is defined as the ratio of the peak production of DCAC

and phosgene to the corresponding degraded TCE. As seen in Fig. 5(a), the yields of DCAC and phosgene in the presence of Pt/$TiO_2$ fell into the range of 10–30% and 4–12%, respectively. The yields of DCAC and phosgene correspond to the $k_{obs}$ of TCE. This indicates that the formation of DCAC and phosgene is subjected to the TCE degradation. The degradation mechanism of TCE over Pt/$TiO_2$ is likely to be the same as that of P25 $TiO_2$. The phenomenon is consistent with the result provided by Driessen and Grassian [2], who reported that Pt particles were not involved in the photocatalytic oxidation of TCE on Pt/$TiO_2$. The overload of Pt just provides additional recombination centers or causes a shelter effect resulting in an inhibitory effect on the TCE degradation.

With increasing loading amount of Pd species, Pd/$TiO_2$ causes a significant decrease in the yield of DCAC to less than 6%, and an increase in the yield of phosgene in the range of 8–16% (Fig. 5(b)). The dependence of the yields of DCAC and phosgene on Pd shows an interesting phenomenon. Although the presence of Pd significantly retards the TCE degradation, it appreciably enhances the selectivity toward phosgene.

Regarding the mechanism of TCE degradation, the process involves chain reactions initiated by $Cl^\bullet$ (Eq. (2)). $Cl^\bullet$ is expected to react with TCE to form $CHCl_2CCl_2^\bullet$, which immediately transforms to $CHCl_2CCl_2OO^\bullet$, as indicated in Eqs. (3) and (4), respectively. Reaction (5) demonstrates the well-known Russel mechanism of $CHCl_2CCl_2OO^\bullet$, resulting in the formation of oxygenated hydrocarbon radicals, $CHCl_2CCl_2O^\bullet$ [12,13]. It has been confirmed that the selectivity toward DCAC or toward phosgene is dependent on the behavior of $CHCl_2CCl_2O^\bullet$ (Eqs. (6) and (7)), an intermediate radical during TCE degradation.

$$TiO_2 + h\nu \rightarrow e^- + h^+ \quad (1)$$

$$Cl^- + h^+ \rightarrow Cl^\bullet; \qquad O_2 + e^- \rightarrow O_2^{\bullet -} \quad (2)$$

$$CHClCCl_2 \ \ (TCE) + Cl^\bullet \rightarrow CHCl_2CCl_2^\bullet \quad (3)$$

$$CHCl_2CCl_2 + O_2^{\bullet -} \rightarrow CHCl_2CCl_2OO^\bullet \quad (4)$$

$$2CHCl_2CCl_2OO^\bullet \rightarrow 2CHCl_2CCl_2O^\bullet + O_2 \quad (5)$$

$$CHCl_2CCl_2O^\bullet \rightarrow CHCl_2CClO(DCAC) + Cl^\bullet \quad (6)$$

$$CHCl_2CCl_2O^\bullet \rightarrow CCl_2O(Phosgene) + CHCl_2^\bullet \quad (7)$$

As seen in reactions (6) and (7), the abstraction of the Cl atom from $CHCl_2CCl_2O^\bullet$ results in the formation of DCAC while the cleavage of the C–C bond causes the formation of phosgene [6,12,16]. Sanhueza et al. [6] discovered that 90% of degraded TCE would transform to DCAC. Based on the aforementioned results, it can be concluded that the participation of Pd is beneficial to the cleavage of the C–C bond. Besides, the production of $H_2$ and $CO_2$ from oxygenated hydrocarbons in aqueous media involves the cleavage of C–C bonds, C–H bonds, and O–H bonds. Mavrikakis and Barteau [26] have indicated that Pd particles are appropriate for these cleavages. This may be the reason for the increase in the selectivity to phosgene in the presence of Pd. In this regard, the intercalated Pd species make the cleavage of C–C bond within $CHCl_2CCl_2O^\bullet$ easier, even though the bond energy of C–C (83 kcal/mol) is somewhat higher than that of C–Cl (81 kcal/mol), as demonstrated in Scheme 1.

## 4. Conclusion

Pt- and Pd-doped $TiO_2$ were fabricated to investigate the effect of Pt and Pd species on the TCE degradation and on the yields of DCAC and phosgene. Some conclusions obtained from the experimental results are as follows:

1. Both Pt and Pd doped on $TiO_2$ deliver an inhibitory effect on TCE degradation. Especially Pd doped on $TiO_2$ dramatically retards photocatalytic efficiency owing to the intercalation of Pd into the $TiO_2$ lattice.
2. The concentration of surface OH is irrelevant to TCE degradation, suggesting that $OH^\bullet$ is not responsible for TCE degradation. Instead, $Cl^\bullet$ initiates the photocatalysis of TCE.
3. Pd particles enhance the cleavage of C–C bond rather than C–Cl bond within $CHCl_2CCl_2O^\bullet$, being favorable to forming phosgene compared to Pt particles.
4. In terms of the photocatalytic degradation of TCE, the photocatalytic behavior of Pt-doped $TiO_2$ is the same as that of P25 $TiO_2$, whereas Pd-doped $TiO_2$ shows a different one.

## References


[1] A. Linsebigler, C. Rusu, J.T. Yate, J. Am. Chem. Soc. 118 (1996) 5284.
[2] M.D. Driessen, V.H. Grassian, J. Phys. Chem. B 102 (1998) 1418.
[3] S.E. Park, H. Joo, J.W. Kang, Sol. Energy Mater. Sol. Cells 83 (2004) 39.
[4] T. Tanimura, A. Yoshida, S. Yamazaki, Appl. Catal. B: Environ. 61 (2005) 346.
[5] L.A. Dibble, G.B. Raupp, Catal. Lett. 4 (1990) 345.
[6] E. Sanhueza, K. Itoh, M. Murabayashi, Chem. Rev. 76 (1998) 313.
[7] M.R. Nimlos, W.A. Jacoby, D.M. Blake, T.A. Mllne, Environ. Sci. Technol. 27 (1993) 732.
[8] W.A. Jacoby, M.R. Nimlos, D.M. Blake, Environ. Sci. Technol. 28 (1994) 1661.
[9] H. Liu, S. Cheng, J. Zhang, C. Cao, Chemosphere 35 (1997) 2881.
[10] K.H. Wang, H.H. Tsai, Y.H. Hsieh, Chemosphere 36 (1998) 2763.
[11] J.S. Kim, H.K. Joo, T.K. Lee, K. Itoh, M. Murabayashi, J. Catal. 194 (2000) 484.
[12] P.B. Amama, K. Itoh, M. Murabayashi, Appl. Catal. B: Environ. 37 (2002) 321.
[13] P.B. Amama, K. Itoh, M. Murabayashi, J. Mol. Catal. A: Chem. 217 (2004) 109.
[14] M. Kang, J.H. Lee, S.H. Lee, C.H. Chung, K.J. Yoon, K. Ogino, S. Miyata, S.J. Choung, J. Mol. Catal. A: Chem. 193 (2003) 273.
[15] T.K. Lim, S.D. Kim, Chemosphere 54 (2004) 305.
[16] M. Mohseni, Chemosphere 59 (2005) 335.
[17] H.H. Ou, S.L. Lo, J. Hazard. Mater. 146 (2007) 302–308.
[18] J.C. Yu, J. Yu, J. Zhao, Appl. Catal. B: Environ. 36 (2002) 31.
[19] F.B. Li, X.Z. Li, Chemosphere 48 (2002) 1103.
[20] Y. Takasu, R. Unwin, B. Tesche, A.M. Bradshaw, Sur. Sci. 77 (1978) 219.
[21] S.C. Fung, J. Catal. 76 (1982) 225.
[22] D.C. Lee, J.H. Kim, W.J. Kim, J.H. Kang, S.H. Moon, Appl. Catal. A: Gen. 244 (2003) 83.
[23] J. Fan, J. Yates, J. Am. Chem. Soc. 118 (1996) 4686.
[24] W. Li, S. Ismat Shah, C.P. Huang, O. Jung, C. Ni, Mater. Sci. Eng. B 96 (2002) 247.
[25] J. Lee, W. Choi, J. Phys. Chem. B 109 (2005) 7399.
[26] M. Mavrikakis, M.A. Barteau, J. Mol. Catal. A: Chem. 131 (1998) 135.